Finite-size effects for lattice glueball masses

Thomas A. DeGrand
Physics Department, University of Colorado, Boulder, Colorado 80309

Carsten Peterson
Department of Theoretical Physics, University of Lund, Lund, Sweden
(Received 30 June 1986)

We have measured the lattice size dependence of the lightest glueball mass in SU(2) and SU(3) gauge theory at $\beta=2.2$ and 2.3 [SU(2)] and $\beta=6.0$ [SU(3)]. We observe an increase in the glueball mass when the lattice size shrinks below a critical value. The magnitude of this length scale, which we interpret as the physical size of the glueball, is roughly the same for SU(2) and SU(3) when expressed in units of the string tension.

I. INTRODUCTION

This paper describes a study of the effects of a finite lattice size on glueball masses in SU(2) and SU(3) lattice gauge theory. It is important to make systematic studies of finite-size corrections to lattice Monte Carlo determinations of masses for two reasons. The first and most obvious reason is to determine what lattice sizes are safe for extracting hadron masses. A second and more exciting reason is the possibility of using finite-size lattices with periodic boundary conditions in the spatial directions to extract other physical quantities such as coupling constants and scattering amplitudes.

The latter effects have been studied theoretically in great detail by Lüscher,[1] who showed that for a sufficiently large lattice size the excitation masses would be modified by terms essentially due to the interactions of the fields with their image charges arising from lattice periodicity. Parametrizing these interactions in terms of an effective three-point interaction $g^2/4\pi$, Lüscher showed that $\mu(L)$, the mass of an excitation in a box of size L, is given by

$$\mu(L)=\mu(\infty)\left[1-\frac{3g^2}{4\pi}\frac{\exp\left[-\frac{\sqrt{3}}{2}\mu(\infty)L\right]}{\mu(\infty)L}\right], \quad (1.1)$$

where $\mu(\infty)$ is the limiting value of μ for large L. A similar result valid for strong-coupling lattice gauge theory has also been derived by Münster.[2]

In Ref. 3 a Monte Carlo simulation of SU(3) lattice gauge theory was carried out at $\beta=5.7$ for two lattice sizes: $6^3\times16$ and $8^3\times16$. Fitting their data to the two parameters $\mu(\infty)$ and $g^2/4\pi$, the authors of Ref. 3 measured a value of $g^2/4\pi=50$. This number is in agreement with the strong-coupling result of Ref. 2 but is very large compared to the pion-nucleon coupling constant $g_{\pi\pi N}{}^2/4\pi=14$. It is also very difficult to reconcile this number with naive large-N arguments.

Recently Hochberg and Thacker[4] have made a systematic Monte Carlo study of finite-size effects in a solvable nontrivial two-dimensional field theory. They consider the Baxter model, which is a lattice version of the massive Thirring model. This toy theory is very instructive since it has as asymptotic states both free fermions and fermion-fermion bound states. Two salient features emerge from the analysis of the model.

(1) When the lattice size decreases from infinity the bound-state mass *decreases* weakly as a result of the periodic boundary conditions. This phenomenon corresponds to the Lüscher effect, Eq. (1.1)

(2) Further decrease of the lattice size results in an *increase* of the bound-state mass. This phenomenon originates from squeezing the wave function and sets in when the lattice size is smaller than the physical size of the bound state. As the lattice size L shrinks the momentum of the fields rises like $2\pi/L$ and the mass of the bound state also rises.

One should keep in mind that finite lattice size studies of confined objects, e.g., hadron masses, should only be performed down to a certain spatial size. The reason for this is that if the size of any of the directions is sufficiently small the Wilson line operator in that direction develops a nonzero expectation value signaling the confinement-deconfinement phase transition. Hence such lattices would induce unwanted finite-size effects for mass calculations.

The goal of this work is to investigate finite-size effects on glueball masses for SU(2) and SU(3) lattice gauge theory as deep into the continuum as possible. We attempt to establish both the phenomena described above in SU(3) at $\beta=6.0$ and attempt to see the wave-function squeezing (small-L) behavior in SU(2) gauge theory at $\beta=2.2$ and 2.3.

For SU(2) we study lattice sizes 8^4, 10^4, 12^4, 14^4, and 16^4. We observe the wave-function squeezing effect in our data for small L. Because of our choice of boundary conditions, we are unable to investigate the Lüscher effect.

The SU(3) calculation was performed at $\beta=6.0$ on $9^3\times14$, $9^2\times11\times14$, $9^2\times13\times14$, $11^3\times14$, $13^2\times11\times14$, and $13^3\times14$ lattices. This is the highest β value for

which glueball mass calculations have been reported to date. We do not believe that we have seen the lightest glueball state in our simulations. Nevertheless we do see a decrease in the effective glueball mass as the lattice size increases from small to moderate size.

The calculations were performed at comparable length scales. It has been shown that $\sqrt{\sigma}/\Lambda_L = 100$ and $\sqrt{\sigma}/\Lambda_L = 50$ for SU(3) and SU(2), respectively[5] (σ is the string tension, Λ_L is the lattice regularization parameter), so that the lattice spacing for SU(3) at $\beta = 6.0$ roughly corresponds to the lattice spacing for SU(2) at $\beta = 2.4$. We find that the values of the length scales where the squeezing of the wave function dies away are comparable for SU(2) and SU(3). For SU(3) we find when going from $L = 2.5/\sqrt{\sigma}$ to $3/\sqrt{\sigma}$ a rise larger than what Eq. (1.1) predicts when $G = 3g^2/4\pi = 155$ (Ref. 3).

The paper was organized as follows. In Secs. II and III we describe the SU(3) and SU(2) calculations. We discuss our conclusions in Sec. IV.

II. THE SU(3) GLUEBALL MASS

The SU(3) simulations were carried out using the Cyber-205 at the Supercomputer Computations Research Institute at Florida State University. The program used a standard ten-hit Metropolis updating algorithm. It is described in Ref. 6. In the program glueball mass measurements were performed using a source method:[3,7,8] all of the spatially oriented links of the lattice at $t = 0$ were set to the identity. Then the expectation values of various operators ϕ (to be described below) were computed, averaging over all locations at a fixed time slice from the source. The variation in $\phi(t)$ with t can be used to extract a mass. Denoting the source as F and the length of the lattice in the time direction as L, and assuming periodic boundary conditions in the t direction gives

$$\langle \phi(t) \rangle = \frac{\langle F(L) \mid \phi(t) \mid F(0) \rangle}{\langle F(L) \mid F(0) \rangle} . \tag{2.1}$$

Expanding in mass eigenstates, we have

$$\langle \phi(t) \rangle = \frac{\sum_{n,m} \langle F \mid n \rangle \langle n \mid \phi \mid m \rangle \langle m \mid F \rangle \exp[-\mu_n (L-t)] \exp(-\mu_m t)}{\sum_n |\langle F \mid n \rangle|^2 \exp(-\mu_n L)} \tag{2.2}$$

and truncating to the lightest glueball mass μ (in units of the inverse lattice spacing)

$$\langle \phi(t) \rangle \simeq A + B \cosh\mu \left[t - \frac{L}{2} \right] , \tag{2.3}$$

where

$$A = \langle 0 \mid \phi \mid 0 \rangle , \tag{2.4}$$

$$B = \frac{e^{-\mu L/2} \langle 0 \mid \phi \mid 1 \rangle \langle 1 \mid F \rangle}{\langle 0 \mid F \rangle} . \tag{2.5}$$

We have measured expectation values of "block operators." Block operators were first used in Monte Carlo renormalization-group studies.[9] One defines a new link variable $V_\mu(x)$ which exists over a longer distance scale than the original links $U_\mu(x)$ and represents in a sense the average value of the gauge field over a larger distance scale. For renormalization-group studies the transformation $U_\mu(x) \to V_\mu(x)$ represents a change of scale transformation and can be used for defining renormalized coupling constants and deriving a β function. Our use of blocked operators is somewhat different: if the blocked operator is a complicated function of the original link variables, then a relatively simple function of the V's (a plaquette, for example) may represent a highly complex function of the U's. These functions may be useful as antennas for glueball operators at large values of β.

Our prescription for introducing a blocked link as as follows. On every other link of the lattice we introduce a variable $V_\mu(x)$. For each lattice configuration we wish to compute V's by maximizing the quantity $\mathrm{Tr} V R^\dagger + \mathrm{H.c.}$ We do this by selecting V's stochastically with a probability

$$P(V_\mu(x)) = \exp\left[\frac{\gamma}{3} (\mathrm{Tr} V R^\dagger + \mathrm{H.c.}) \right] , \tag{2.6}$$

where R is the sum of products of U's over the path of length 2 connecting the points at x and $x + 2\hat{\mu}$:

$$R_1 = U_\mu(x) U_\mu(x + \hat{\mu}) \tag{2.7}$$

and the six paths of length four:

$$R_2 = \sum_{\pm \nu \neq \mu} U_\nu^\dagger(x) U_\mu^\dagger(x + \hat{\nu}) U_\mu^\dagger(x + \hat{\nu} + \hat{\mu}) U_\nu(x + 2\hat{\mu}) . \tag{2.8}$$

Our prescription for computing Eq. (2.6) is to begin by setting $V_\mu(x) = R_1$ and then to include R_2 in (2.6) and carry out ten Metropolis hits with a large value of γ (typically, $\gamma = 30$). We repeat this procedure for all V's and then measure spacelike and space-time orientations of all 1×1 V-plaquettes:

$$V_{\mu\nu} = \langle \mathrm{Tr} V_\mu(x) V(x + 2\hat{\mu}) V_\mu^\dagger(x + 2\hat{\nu}) V_\nu^\dagger(x) \rangle . \tag{2.9}$$

The reader can easily convince himself that this 1×1 plaquette, written in terms of the original variables, is a superposition of many shapes of loops ranging in surface area from 0 to 12 plaquettes in size.

We must remark that we have made no attempt to optimize our operators as glueball antennas. That optimization can only be done using a variational calculation, that is, by measuring correlations of operators with each other rather than with a source. In retrospect, this would have been a good thing to do before carrying out the finite-size calculation. We hope to return to it later. Even without optimizing, we find that the block operators are somewhat

TABLE I. SU(3) masses, $\beta=6$, $t_{\min}=3$. We quote lattice masses from blocked space-time and blocked space-space plaquettes separately.

Lattice size	s-t plaquettes	s-s plaquettes	Sweeps
9^3	1.62±0.10	1.27±0.10	15000
$9^3\times 11$	1.40±0.06	0.92±0.12	15000
$9^3\times 13$	1.47±0.07	1.13±0.15	16000
11^3	1.19±0.07	0.87±0.08	15000
$13^2\times 11$	1.39±0.08	1.41±0.10	10000
13^3	1.45±0.06	1.21±0.11	9000

less noisy than, for example, the simple 2×2 Wilson loops.

All of the SU(3) data are from runs at $\beta=6$. The lattice size ranges from $9^3\times 14$ to $13^3\times 14$ and at each value of lattice size 10000 to 15000 sweeps of the lattice were performed.

A common problem in lattice mass calculations is determining if or when the correlation function is dominated by its lowest-mass excitation, Eq. (2.3). If the coupling of the source to that state is sufficiently small, the state may not be seen in $\langle\phi(t)\rangle$. For example, the 1×1 plaquette is known to couple very poorly to the lightest glueball state at $\beta=5.9$ (Ref. 3). As a symptom of this disease, the values for μ computed by beginning the fit at different separations from the source will drift with the separation. In addition, as the fitting is carried out farther and farther from the source, the mass is determined with less and less precision since the variation in the hyperbolic cosine shrinks. If the variation in the mass with $t_{\min}$ has not ceased by the time the signal has gone into the noise, then one cannot be certain that one has not measured the asymptotic falloff of $\phi(t)$.

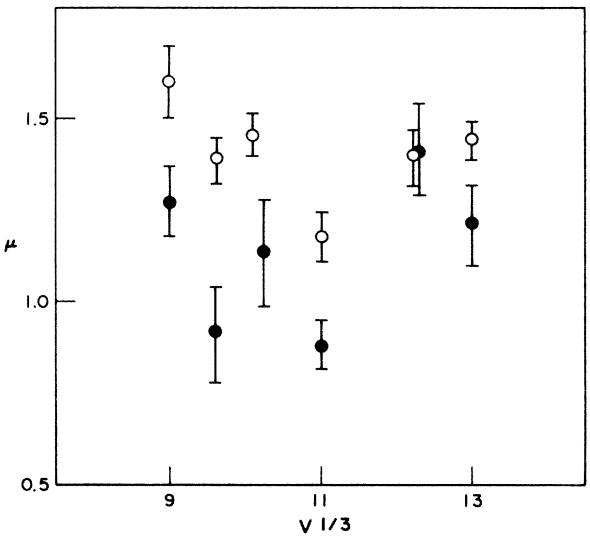

FIG. 1. SU(3) glueball masses at $\beta=6$ beginning at $t_{\min}=3$ sites from a hot-wall source, vs the lattice size $V^{1/3}=(N_xN_yN_z)^{1/3}$. Open circles are blocked space-time plaquettes, closed circles are blocked space-space plaquettes.

Unfortunately that is the case for our SU(3) data. The crossover point, where the fractional error on the mass approaches 25%, is at $t_{\min}=4$ lattice spacings. In order to have a signal which shows measurable variation with the size of the lattice, we choose to present masses from fits beginning at $t_{\min}=3$ lattice spacings from the origin. In consequence, we do not claim that we are seeing the lightest glueball in our data, in contrast with the situation for SU(2).

Our SU(3) data are shown in Table I. The mass is plotted in Fig. 1 as a function of lattice size $R=(N_xN_yN_z)^{1/3}$. Both blocked space-time and blocked space-space plaquettes show a drop from $R=9$ to $R=11$ followed by a rise to the $R=13$ point. The asymmetrically sized lattices interpolate between these points. The observed lattice size dependence of μa will be discussed in Sec. IV.

III. THE SU(2) GLUEBALL MASS

A. Numerical method

For measuring the SU(2) glueball mass we have employed the fixed boundary method of Ref. 8. This method is an ultimate extension of the fixed wall method used above. Here one measures the response of plaquettes inside concentric hypercubes inside an L^4 hypercube to the change in boundary conditions. The reader is referred to Ref. 8 for details. The first step is to measure the differences $\Delta(d)$ of the average plaquettes inside $(L-d)^4$ cubes for two different boundary conditions. The differences $\Delta(d)$ can be expressed as a sum over all correlations between the plaquettes on the boundary (P) and those inside the $(L-d)^4$ cube (Q):

$$\Delta(d)\simeq\sum_{P,Q}\rho(P,Q)\ , \tag{3.1}$$

where $\rho(P,Q)$ is expected to take the form

$$\rho(P,Q)=e^{-r(P,Q)/\xi}\ . \tag{3.2}$$

Here $\xi=1/\mu$ is the correlation length and $r(P,Q)$ the Euclidean distance between the plaquettes P and Q. μ is extracted from Eqs. (3.1) and (3.2) by forming ratios $\Delta(d)/\Delta(d-1)$ thereby canceling the normalization factor in Eq. (3.1). Since all plaquettes inside the $(L-d)^4$ hypercube are measured one is actually probing an effective distance $\hat{d}>d$.

What are the advantages and disadvantages of this method?

(1) Clearly the method is extremely efficient since one

creates an optimal number of enhanced correlations; it utilizes walls in all four directions. The method does not project out particular angular momentum or spin eigenstates. As in the case of the wall method described in Sec. II the mass derived with this method is not a rigorous lower bound.

(2) For our purposes this algorithm has the disadvantage of not allowing for glueball-glueball interactions (the Lüscher effect) since one does not have periodic boundary conditions in the spatial directions. However effects from squeezing the wave function should still be there.

B. Monte Carlo calculations

We have performed Monte Carlo calculations for $\beta=2.2$ and 2.3 with lattice sizes 8^4, 10^4, 12^4, 14^4, and 16^4 using the Metropolis algorithm with three updatings per link with the icosahedral subgroup. For these couplings $d=3$ turns out to be sufficient for making asymptotic measurements. We have checked that the $d=4$ results are consistent with $d=3$ within the errors for $\beta=2.3$ but stick to $d=3$ in order to obtain better statistics. Further improvement on the statistics was obtained by updating the innermost cubes more frequently than the outer ones. The relative frequencies were chosen 1:5:25 for cubes at distances 1, 2, and 3 from the boundary. Further details of the Monte Carlo runs are shown in Table II together with the measured differences $\Delta(d)$ and the extracted masses.

The average plaquettes P, when measured with periodic boundary conditions, exhibit no variation over the different sizes. We have therefore for each β averaged P from all the lattice sizes in order to reduce the errors.

In Fig. 2 we show how μ varies with L for $\beta=2.2$ and 2.3. These results will be discussed in the next section.

IV. DISCUSSION OF THE RESULTS

We can most easily compare the SU(2) and SU(3) data by normalizing them to the string tension. First we write the two-loop expression for the lattice spacing [$\beta=2N/g^2$ for SU(N)]:

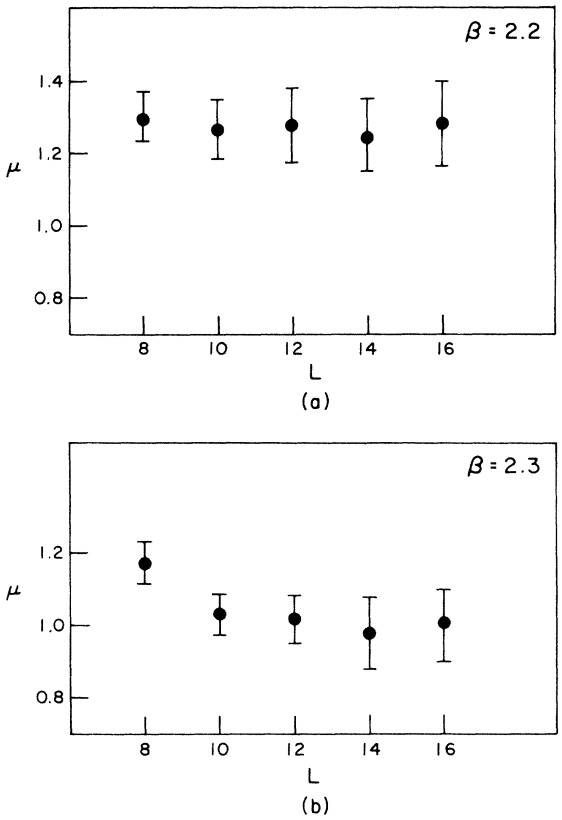

FIG. 2. SU(2) glueball masses vs lattice size. (a) $\beta=2.2$. (b) $\beta=2.3$.

$$a\Lambda_L=\left[\frac{24\pi^2}{11N^2}\right]^{51/121}\exp\left[-\frac{12\pi^2}{11N^2}\beta\right]. \tag{4.1}$$

One has $a\Lambda_L=0.0023$ [SU(3),$\beta=6.0$], 0.0076 [SU(2), $\beta=2.2$], and 0.0060 [SU(2), $\beta=2.2$]. A recent analysis gives $\sqrt{\sigma}/\Lambda_L=95$ [SU(3)] and 50 [SU(2)] (Ref. 5). Thus the lattice spacing in units of the string tension is $a\sqrt{\sigma}=0.22$ [SU(3)], 0.38 and 0.30 [SU(2), $\beta=2.2$ and

TABLE II. (a) Measured masses in SU(2) at $\beta=2.2$ We display separately the number of sweeps used for thermalization and the number of sweeps for the innermost cubes of the lattice. (b) SU(3) masses, $\beta=2.3$.

Lattice size	Thermal sweeps	Inner sweeps	μ
	(a)		
8^4	1500	25 000	1.30±0.07
10^4	1500	13 000	1.27±0.08
12^4	2000	4 000	1.28±0.10
14^4	3000	2 500	1.24±0.11
16^4	3000	1 250	1.28±0.12
	(b)		
8^4	($\beta=2.2$)+1500	25 000	1.17±0.05
10^4	($\beta=2.2$)+1500	25 000	1.03±0.05
12^4	($\beta=2.2$)+2000	7 500	1.01±0.07
14^4	($\beta=2.2$)+3000	2 500	0.98±0.10
16^4	($\beta=2.2$)+3000	1 250	1.00±0.10

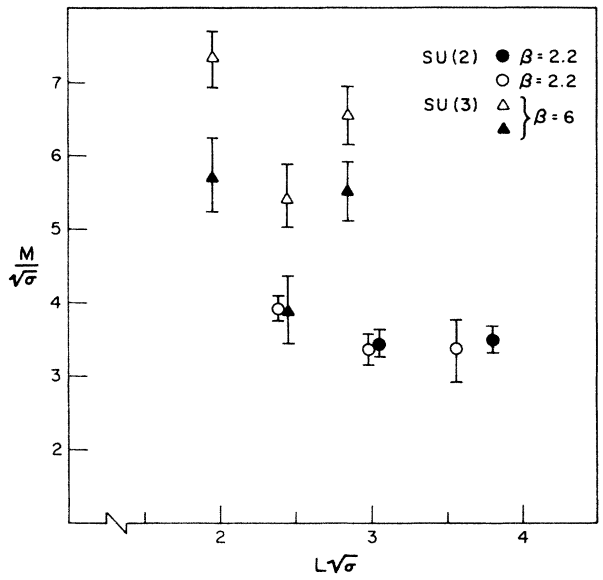

FIG. 3. Comparison of SU(2) and SU(3) results (the latter on symmetric lattices). Mass and length are expressed in units of $1/\sqrt{\sigma}$. Open and closed circles are SU(2) with $\beta=2.3$ and 2.2, respectively; open and closed triangles are $\beta=6$ SU(3) measurements of space-time and space-space plaquettes, respectively.

2.3]. We plot the SU(2) and SU(3) masses (in units of $\sqrt{\sigma}$) for symmetric lattices and for short distances (in units of $1/\sqrt{\sigma}$) in Fig. 3.

The $\beta=2.2$ SU(2) masses show no variation with size while the $\beta=2.3$ mass decreases in going from an 8^4 lattice to a 10^4 lattice and then holds constant. These results are internally consistent: the $L=8$ lattice at $\beta=2.2$ has the same physical size as the $L=10$ lattice at $\beta=2.3$. It appears that for SU(2) the lattice size for which squeezing of the wave function sets in is $L\simeq 3/\sqrt{\sigma}$.

These numbers represent continuum physics. Mütter and Schilling have shown that the SU(2) glueball masses scale for $\beta>2.2$ (Ref. 8) and our data for $\beta=2.2$ and 2.3 confirm their result. We find

$$\frac{m}{\sqrt{\sigma}}=3.4\pm 0.3 \ . \tag{4.2}$$

Note that the continuum glueball radius is not equal to the glueball Compton wavelength: $mL\simeq 10$. More detailed measurements of the properties of SU(2) glueball wave functions would require techniques other than the totally fixed boundary conditions we have employed in this work. This is an obvious project for future studies.

The SU(3) masses are almost twice as high as their SU(2) counterparts and probably do not represent the lightest glueball state. Nevertheless, they also show a decrease from $L=2/\sqrt{\sigma}$ to $L=2.5/\sqrt{\sigma}$.

The SU(2) and SU(3) data at large L are expected to be, and are found to be, considerably different from one another. The SU(2) simulations are performed with fixed boundary conditions, for which there is no analog of the Lüscher effect since the gauge fields cannot relax into a band. The SU(3) calculations are performed on a system

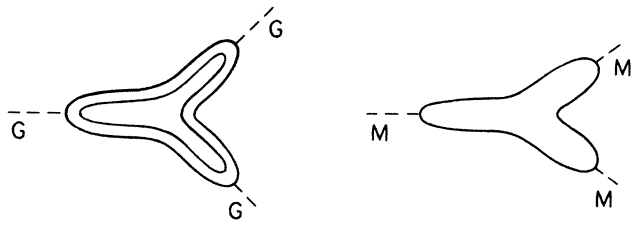

FIG. 4. (a) The lowest-order graph for the three-glueball system. (b) The lowest-order graph for the three-meson system.

with skew periodic boundary conditions and can in principle show a Lüscher effect. However, the magnitude of the rise in μ which we see in going from $L=2.5/\sqrt{\sigma}$ to $L=3/\sqrt{\sigma}$ is much larger than the asymptotic value of that effect. As an illustration, taking the parametrization of Ref. 3,

$$\mu(L)=\mu(\infty)\left[1-G\frac{\exp\left[-\frac{\sqrt{3}}{2}\mu(\infty)L\right]}{\mu(\infty)L}\right] \tag{4.3}$$

plus their value of $G=155$ and $\mu\simeq 1$ gives a correction to the mass at $L=11$ of $\Delta\mu/\mu\simeq 10^{-3}$.

The change in μ at large L is comparable to or larger than that seen by Ref. 3. This result implies that either at $\beta=6$, G is a factor of 10^4 larger than was seen by Ref. 3, or else the variation in $\mu(L)$ cannot be explained using Eq. (1.1). It is likely that the second possibility is the correct one. Equation (1.1) is meant to be applicable when the lattice size is very large compared to the size of the glueball, and yet we know from our observation of wave-function squeezing that our largest lattice is probably not much bigger than the glueball diameter.

A large triple-glueball coupling constant is somewhat unexpected from large-N arguments. With $M_{G\to gg}\simeq 1/N$ one has [see Fig. 4(a)]

$$M_{G\to GG}\simeq\frac{1}{N^3}N^2=\frac{1}{N} \ . \tag{4.4}$$

Correspondingly for the mesonic couplings one gets, with $M_{M\to qq}\simeq 1/\sqrt{N}$ [see Fig. 4(b)],

$$M_{M\to MM}\simeq\frac{1}{(\sqrt{N})^3}N=\frac{1}{\sqrt{N}} \ . \tag{4.5}$$

Hence hadron-hadron couplings should be suppressed in the gluonic sector as compared to the quark sector.

We can draw two conclusions from our data; both are related to the squeezing of the wave function at shorter distances. First, the minimum size lattice, to avoid seeing finite-size effects, is expected to change with β, presumably according to the renormalization group, for large enough β. As a practical consideration, if one wishes to perform Monte Carlo simulation at other values of β, one must have a large enough lattice so that one's mass is not lattice size dependent. Taking $L=8$ for SU(2) at $\beta=2.2$ and $L=11$ for SU(3) at $\beta=6.0$, we illustrate in Table III the variation of $L_{\min}$ over the currently computationally interesting values of β.

TABLE III. Minimal lattice size L_m required in order to avoid the squeezing effect in SU(2) and SU(3) for different β values.

SU(2)	β	2.2	2.3	2.4	2.5	2.6
	$L_{\min}$	8	10	14	17	22
SU(3)	β	5.9	6.0	6.1	6.2	6.3
	$L_{\min}$	10	11	13	14	16

The second conclusion relates to the applicability of our results for SU(3) to continuum physics. We do not believe that we are seeing the true asymptotic behavior of $\langle\phi(t)\rangle$. The mass we extract is large, compared both to the SU(2) glueball mass (in units of the string tension) and to glueball masses measured at lower values of β (in lattice units). Furthermore, it appears that the two operators we have measured couple to a different mixture of glueball states since the masses we extract are different. Since the source method is not variational we cannot argue from first principles that our results provide an upper bound on the true glueball mass. However, experience at lower β indicates that glueball masses measured using the hot-wall source tend to approach their asymptotic value from above as $t_{\min}$ increases.

Our results are still interesting from the point of view of wave-function size. The lightest glueball is unlikely to have a size smaller than around four lattice spacings at $\beta=6$, or else our operators would couple more efficiently to it. Excited state glueballs are likely to have larger radii than the ground state since that is the case for nearly all quantum-mechanical bound states. The fact that masses extracted from both our operators show an increase for $L<11$ or so is a signal that glueballs with a mass around $6\sqrt{\sigma}-7\sqrt{\sigma}$ have a diameter of around 9–11 lattice spacings, and that this number is not strongly dependent on the degree of excitation of the glueball. Taking $\sqrt{\sigma}=400$ MeV, this estimate gives a physical diameter for a 2400-MeV glueball of around 1.2 fm, a "typical" hadronic diameter.

The glueball size which we infer from our data is similar to the quark hadronic sizes measured in Ref. 10. In quenched approximation and at $\beta=5.7$, the authors of Ref. 10 determined that the proton, Δ, and pion wave functions peaked at a diameter of around four lattice spacings and extended out to around eight lattice spacings. Assuming scaling (which may not be justified) one lattice spacing is $0.31/\sqrt{\sigma}$ and eight lattice spacings is again 1.24 fm. From the point of view of size the glueball appears to be a typical hadron.

ACKNOWLEDGMENTS

C.P. acknowledges the Physics Department at the University of Colorado for its hospitality when this project was launched. T.D. would like to thank the Department of Theoretical Physics of Lund University for its hospitality during the completion of this work. He was also supported by the U.S. Department of Energy and by NORDITA.

[1]M. Lüscher, in *Progress in Gauge Field Theory,* proceedings of the Cargese Summer Institute, Cargese, France, 1983, edited by G. 't Hooft *et al.* (NATO Advanced Study Institute, Series B: Physics, Vol. 115) (Plenum, New York, 1984); Commun. Math. Phys. **104**, 177 (1986).

[2]G. Münster, Nucl. Phys. **B249**, 659 (1985).

[3]P. de Forcrand, G. Schierholz, H. Schneider, and M. Teper, Phys. Lett. **152B**, 107 (1985).

[4]D. Hochberg and H. Thacker, Nucl. Phys. **B257** [FS14], 729 (1985).

[5]M. Flensberg and C. Peterson, Lund Report No. LU TP 85-14 (unpublished).

[6]T. DeGrand and C. DeTar, Phys. Rev. D **34**, 2469 (1986).

[7]C. Michael and I. Teasdale, Nucl. Phys. **B225**, 933 (1983).

[8]K. Mütter and K. Schilling, Phys. Lett. **117B**, 75 (1982).

[9]K. C. Bowler *et al.*, Nucl. Phys. **B257** [FS14], 155 (1985).

[10]S. Gottlieb, in *Advances in Lattice Gauge Theory,* edited by D. Duke (World Scientific, Singapore, 1985).